Electrocatalytic Oxidation of Ethanol and Ethylene Glycol onto Poly (*o*-Anisidine)-Nickel Composite Electrode

Naddaf, Ezzat*+; Abedi, Mohammad Reza
Department of Applied Chemistry, Quchan Branch, Islamic Azad University, Quchan, I.R. IRAN

Zabihi, Mohammad Saleh
Department of Applied Chemistry, North Tehran Branch, Islamic Azad University, Tehran, I.R. IRAN

Imani, Alihossien
Young Researchers Club, Quchan Branch, Islamic Azad University, Quchan, I.R. IRAN

ABSTRACT: *In this work, poly (o-Anisidine) (POA) was prepared by consecutive potential cycling in an acidic monomer solution at the surface of Carbon Paste Electrode (CPE). Nickel ions were dispersed into the polymer by immersing the electrode in NiSO$_4$ solution. The prepared Ni/POA/CPE was characterized by scanning electron microscopy, energy dispersive X-ray spectroscopy, Atomic Force Microscopy (AFM) and electrochemical methods. The electrochemical oxidation of ethanol and ethylene glycol was investigated at the Ni/POA/CPE by cyclic voltammetry and chronoamperometry techniques. The results indicated that the Ni/POA/CPE in comparison with Ni/CPE exhibited excellent electrocatalytic activity towards oxidation. Then, using a chronoamperometry method, the catalytic rate constant, k, for ethanol and ethylene glycol oxidation were found to be 2.6×10^6 and 1.07×10^7 cm^3/mol s, respectively. Furthermore, the effect of several parameters such as OA concentration, POA thickness, and NiSO$_4$ concentration and accumulation times towards the ethanol oxidation as well as the long-term stability of the modified electrode has been investigated.*

KEYWORDS: *Poly (o-Anisidine); Nickel; Ethylene glycol; Ethanol; Electrocatalytic oxidation.*

INTRODUCTION

Direct Alcohol Fuel Cell (DAFC) is a new source of energy that has recently attracted much attention in the search for alternative energy resources. The alcohols that are used as fuel in DAFCs are methanol, ethanol, ethylene glycol and 2-propanol [1, 2]. The direct oxidation of methanol in fuel cells has been widely investigated. However, the question of the toxicity of methanol remains crucial. Ethanol offers an attractive alternative as a fuel because it can be produced in large quantities from agricultural products and it is the major renewable biofuel from the fermentation of biomass [3, 4]. In contrast to the much studied hydrogen-oxygen fuel cell, ethanol provides a volumetric energy density that approaches that of gasoline. As a liquid fuel, ethanol also

avoids issues of storage associated with proposed hydrogen systems. Ethylene glycol, due to its higher energy density, lower flammability, lower toxicity, and lower permeation through the membrane compared to methanol, has been considered for direct alcohol fuel cell applications [5-7].

In alkaline media, DAFCs show better polarization characteristics in the oxidation of methanol on platinum than in acidic media [8]. Furthermore, using alkaline electrolytes allows for a greater possibility for application of non-noble and less expensive metal catalysts. By the way, alcohol permeation rate are reduced by the reversing of the direction of ionic current due to hydroxide ion conduction against conventional proton conducting system [1, 9, 10]. These reasons motivate investigations on ethanol and ethylene glycol electrooxidation in order to improve the electrical performances when using it in a direct ethanol and ethylene glycol fuel cell, and to open the possibility of replacing methanol in a direct alcohol fuel cell [11-17].

Platinum-based catalysts have been used as the best catalysts [18]. However, they still suffer from multiple problems such as slow reaction kinetics, CO poisoning, high cost, limited reserve in nature, and poor durability [19-21]. For reducing the usage of the precious Pt metal and here after the cost of FCs, the progress of non-Pt electrocatalysts has thus generated an enormous interest [22]. Alternatively, nickel is a promising catalyst because it is cheaper than Pt and has a higher catalytic activity for small alcohols. Several investigations on electrooxidation of the alcohols on Ni have already been reported [23-26].

Conducting polymers offer great advances due to their very good conducting and mechanical properties and good adhesion to the electrode substrate. Therefore, it is of interest to extend such studies to other polymers which might be suitable as host materials for the catalyst micro particles, especially on low price substrate. On the other hand, the easy and fast preparation, low background current, wide potential window, porous and reproducible surface, and low cost of Carbon Paste Electrode (CPE) have been motivated the researchers to use the electrode substrate for deposition of the conducting polymers [27].

In the present study, poly (*o*-Anisidine) (POA) was prepared by electropolymerization of monomer solution at the CPE surface. Ni was then incorporated into the polymer by the accumulation of Ni(II) from NiSO$_4$ solution at open circuit condition. Surprisingly, the literature survey indicates that there is no report as yet on electrocatalytic oxidation of ethanol and ethylene glycol. Therefore, POA modified CPE, which is a conductive organic matrix, was prepared and allowed a better dispersion of Ni ions as a catalyst for the alcohol electrooxidation.

EXPERIMENTAL SECTION
Materials

The solvent used in this work was double distilled water. H$_2$SO$_4$ (98%, Merck) and NaOH(>99%, Merck) were used as the supporting electrolytes. The NiSO$_4$·6H$_2$O (98%,Fluka),OA monomer (>98%, Fluka) were used as received. Ethanol (Merck) and ethylene glycol (Merck) used in this work were analytical grade.K$_3$Fe(CN)$_6$ (>99%, Merck),K$_4$Fe(CN)$_6$ (>99%, Merck) and KCl (>99%, Merck) were used for the electrochemical impedance study. High viscosity paraffin oil (density: 0.86 g cm^{-3}, Merck) was used as pasting liquid in the preparation of the CPE. Graphite powder (particle diameter: 0.1 mm, Merck) was used as the working electrode substrate.

Instrumentation

The surface morphology and elemental analysis were performed by Scanning Electron Microscopy (SEM, model KYKY-EM3200, China), Energy Dispersive Spectrometer (EDS, VEGA-Tescan, Razi Metallurgical Research Center, Tehran, Iran) and Atomic Force Microscopy (AFM, model no. 0101/A, Ara Research company, Iran) respectively. The electrochemical experiments such as Cyclic Voltammetry (CV), chronoamperometry and Electrochemical Impedance Spectroscopy (EIS) were carried out using potentiostat/galvanostat AUTOLAB PGSTAT 30 electrochemical analysis system and GPES 4.9 software package (Eco Chemie, Netherlands) coupled with a personal computer. The utilized three-electrode system was composed of Ag|AgCl|KCl (3M) as reference electrode, a platinum wire as auxiliary electrode, unmodified carbon paste and modified carbon paste (3.9 mm in diameter) as working electrodes. All potentials reported in this work are referenced to the Ag|AgCl|KCl (3M). All experiments were conducted at ambient temperature.

Working electrode preparation

Fabrication of the CPE was performed by mixing graphite powder and paraffin oil in a ratio of 70:30 (%w/w). Using a syringe, paraffin oil was added to the mixture and mixed well until a uniformly wetted paste was obtained. The resulting paste was then inserted into the bottom of a glass tube (internal radius: 3.9 mm). The electrical connection was implemented by a copper wire lead fitted into the glass tube. A fresh electrode surface was generated rapidly by extruding a small plug of the paste out of the tube and smoothing the resulting surface on white paper until a smooth shiny surface was observed. Then, CV was performed between 0.0 and 1.0 V at 50 mV/s in 0.5 M H_2SO_4 solution, until stable CVs were obtained. The modification was performed in three steps:

(a) Electrochemical polymerization of 2.0 mM OA monomer in 0.5 M H_2SO_4 solution by using consecutive potential cycling (10 cycles at v = 50 mV/s) between 0.0 and 1.2 V.

(b) Incorporation of Ni^{2+} (as inexpensive metallic ions) to the POA/CPE by immersing the freshly electro-polymerized CPE in a well-stirred aqueous 0.1M $NiSO_4$ solution for accumulation time of 1 min.

(c) After Ni^{2+}incorporation due to the complex formation between Ni^{2+} and amines sites in the polymer backbone, the electrode was rinsed with distilled water. At beginning of experiment, the Ni/POA/CPE was immersed in 0.1M NaOH solution and the potential was cycled between 0.1 to 0.8V at v = 50 mV/s until reproducible CVs were attained (10 cycles). This technique allows the oxide/hydroxide film formation in parallel with inspecting the electrochemical reactivity of the surface.

Table 1 summarizes several surface parameters such as geometric surface area, polymer mass, film thickness, the surface coverage of nickel hydroxide, anodic electron transfer coefficient and electron transfer rate constant for the Ni/POA/CPE.

Mass of polymer is obtained by $\eta Q_{dep}M/Fn$ equation. Q_{dep} is the sum of monomer charges, assuming 100% polymerization efficiency mass of polymer calculated 2.26 μg. In order to calculate the thickness of polymer, the mass of polymer is divided by density and geometric area.

Ni surface coverage on the carbon paste electrode polymerized by o-anisidine is derived from the charge

Table 1: Surface parameters of the Ni/POA/CPE.

Surface parameter	Value
Geometric area, A_g , cm^2 (πr^2)	0.125
POA mass, W_{POA} , μg ($\eta Q_{dep}M/Fn$)	2.26
POA thickness, d_n , μm ($\eta Q_{dep}M/\rho A_g Fn$)	0.12
Ni loading, W_{Ni} , mg/cm^2	1.05
Surface coverage, Γ_{POA}, mol/cm^2 ($4RTI_p/n^2F^2vA_g$)	9.8×10^{-8}
Surface coverage, Γ_{Ni}, mol/cm^2	1.79×10^{-5}
*Anodic electron transfer coefficient, α	0.73
**Apparent charge transfer rate constant, k_s, s^{-1}	0.055

$^*E_{pa} = E^0 + A\ ln\ [(1 - \alpha)/m],\ E_{pc} = E^0 + B\ ln\ [\alpha/m],$
$A = RT/(1-\alpha)nF, B = RT/\alpha nF,\ m = (RT/F)(k_s/nv)$
$^{**}log\ k_s = \alpha\ log\ (1 - \alpha) + (1 - \alpha)\ log\alpha - log\ (RT/nFv) - [\alpha\ (1-\alpha)$
$nF\Delta E_p]/2.3RT$

under the current–potential curve that is calculated by correction of the baseline ($\Gamma * = Q/nFA$).

The transfer coefficient (α) and apparent charge transfer rate constant, k_s is obtained from plot of peak potential with scan rate that results in extracting two straight lines with slopes equal to 2.3RT/nF and 2.3RT/(1−α)nF for the cathode and anodic peak according to ref 28.

RESULTS AND DISCUSSION

Electrochemical polymerization

In this work, electropolymerization of the OA monomer was investigated at the surface of CPE. The consecutive CVs recorded during the polymerization were presented in Fig. 1. As it can be seen in this figure, on the 1st cycle, a peak related to the OA oxidation at 0.84 V appears and deposition a part of the oxidation products leads to create a POA film at the electrode surface. It is obvious that by continuous potential cycling, this peak shifts towards more positive directions and its height decrease due to loss of the surface activity. As the CVs continue, the peak current densities related to the oxidation and reduction of the polymer are gradually increased. After polymerization, the polymer modified electrode was washed with double distilled water and the potential was cycled between 0.0 and 1.2 V (10 cycles at v = 50 mV/s) in 0.5 M H_2SO_4 solution. The purpose is to remove the monomers and/or oligomers in the polymer film. The stability of prepared films shows decreasing
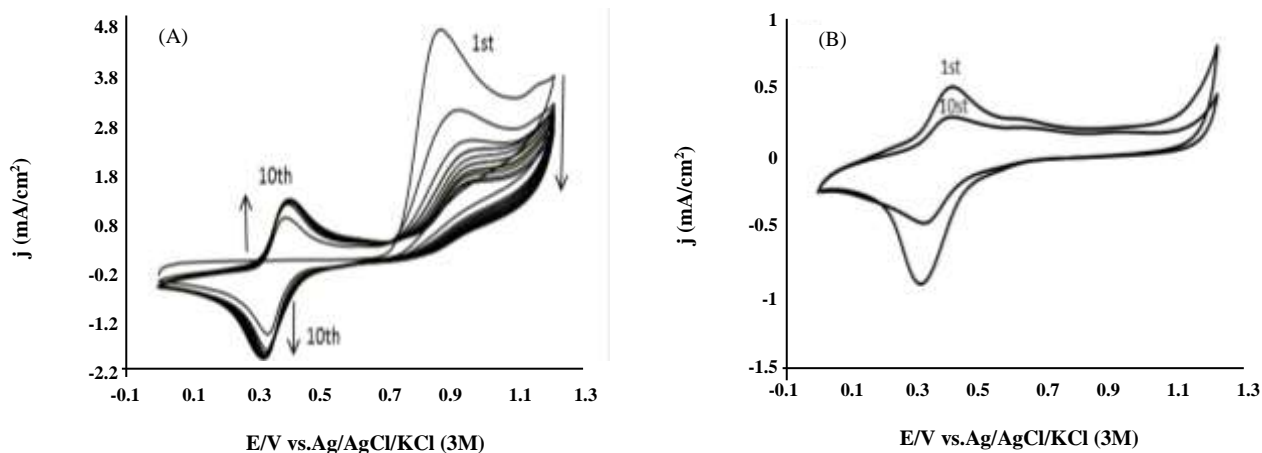
Fig. 1: (A) Electropolymerization of the 2.0 mM OA monomer in 0.5 M H₂SO₄ solution at the surface of CPE at υ = 50 mV/s. (B) CVs of the POA/CPE in 0.5 M H₂SO₄ solution: 1ˢᵗ cycle (a); 10ᵗʰ cycle (b) at υ = 50 mV/s.
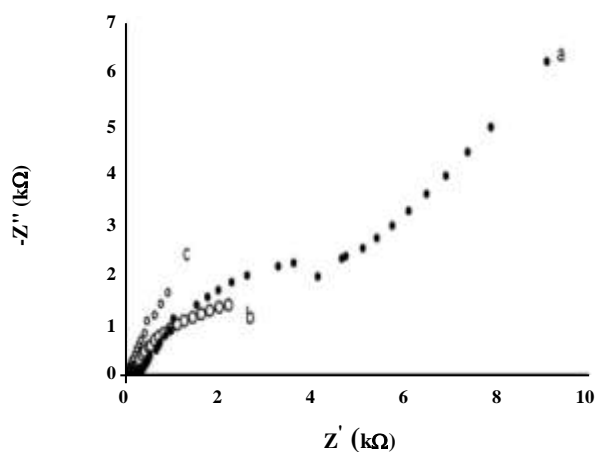

Fig. 2: Niquist plots of the faradaic impedance measurements of a 1.0 mM K₃[Fe(CN)₆]/K₄[Fe(CN)₆] + 0.1 M KCl solution performed on (a) CPE, (b) POA/CPE and (c) Ni/POA/CPE at open circuit potential.

in current at initial 10 cycles and the current almost remains constant afterward (Fig. 1B).The ΔE_p (= 29 mV) for the redox peak is close to 59/n mV, which identifies that the number of involved electrons is 2 ($n \approx 2.03$). The ratio of anodic to cathodic peak current density (j_{pa}/j_{pc}) is almost equal to unity.

EIS studies

EIS is an effective tool for studying the interface properties of polymer-modified electrodes. The typical impedance spectrum (presented in the form of the Nyquist plot) includes a semicircle portion at higher frequencies corresponding to the limited electron-transfer process and a linear part at lower frequency range representing the diffusion-limited process [31]. The semicircle diameter in the impedance spectrum equals the electron-transfer resistance, R_{et}. This resistance controls the electron-transfer kinetics of the redox probe at the electrode interface. Therefore, R_{et} can be used to describe the interface properties of the electrode. The Nyquist diagrams of the CPE (curve a), POA/CPE (curve b) and Ni/POA/CPE (curve c) in the presence of 1.0 mM K₃ [Fe(CN)₆]/K₄[Fe(CN)₆] (1:1) + 0.1 M KCl solution were shown in Fig. 2. As shown in this figure, the value of R_{et} for the POA/CPE is much smaller than that the CPE indicating a faster electron-transfer process on polymeric modified electrode. This may be attributed to the higher real surface area and/or positively charged polymeric skeletons immobilized on the electrode surface which shows an attraction force to ferro/fercyanidean ions. On the other hand, R_{et} at the Ni/POA/CPE shows the smallest value among the other electrodes due to the presence of nickel species.

Surface morphology and elemental analysis

In order to surface characterization, the micrographs of the POA/CPE (a) and Ni/POA/CPE (b) have been investigated by SEM and the corresponding results were shown in Fig. 3. As shown in trace (a), POA film shows an almost rough surface with holes or cavities.
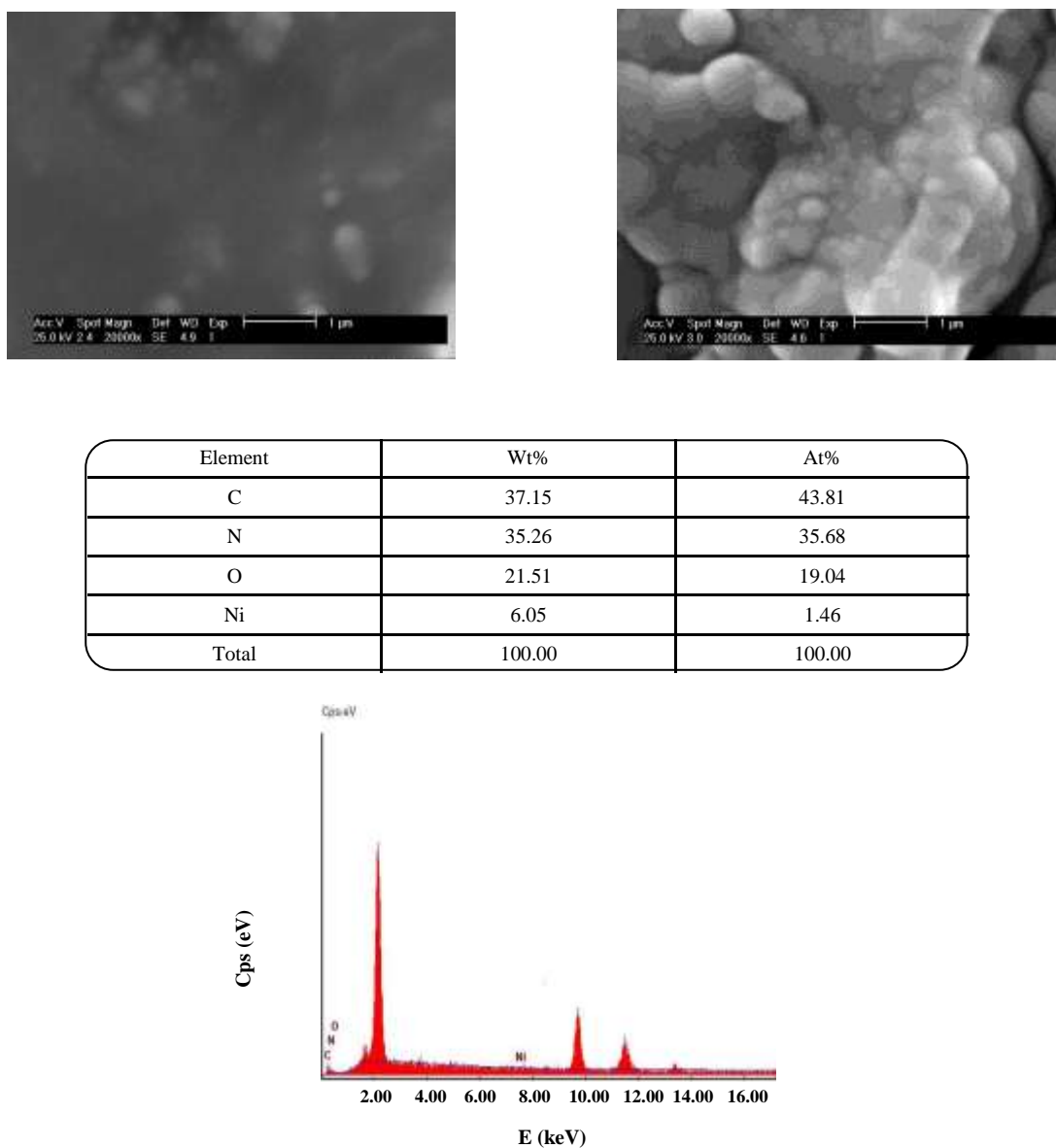
Element	Wt%	At%
C	37.15	43.81
N	35.26	35.68
O	21.51	19.04
Ni	6.05	1.46
Total	100.00	100.00

Fig. 3: SEM images of the (a) POA/CPE and (b) Ni/POA/CPE. (c) EDS spectrum of the Ni/POA/CPE.

This structure enhances the electrolyte constituent access to the interior of the polymeric film. Figure 3b exhibits the POA film formed in the presence of Ni which has amorphous like surface with poly disperse morphology. Furthermore, the existence of the Ni particles incorporated into the composite matrix was confirmed by EDS (trace c). From the EDS results, Ni is the major element. Carbon is derived from the CPE and POA film. Nitrogen is from POA. Oxygen is from POA and/or working electrolyte solution.

Characterization surface of Ni/POA/CPE by AFM

Roughness surface parameter Ni/POA/CPE investigated by atomic force microscope. Images were achieved under room temperature using nano probe cantilever in contact mode. Topographic, phase and amplitude 2D and 3D images (Fig. 4) verified by SEM image in Fig. 3(B). The existence of regular and dispersed Nickel on Polymer layers was showed by the topographic image at the electrode surface.
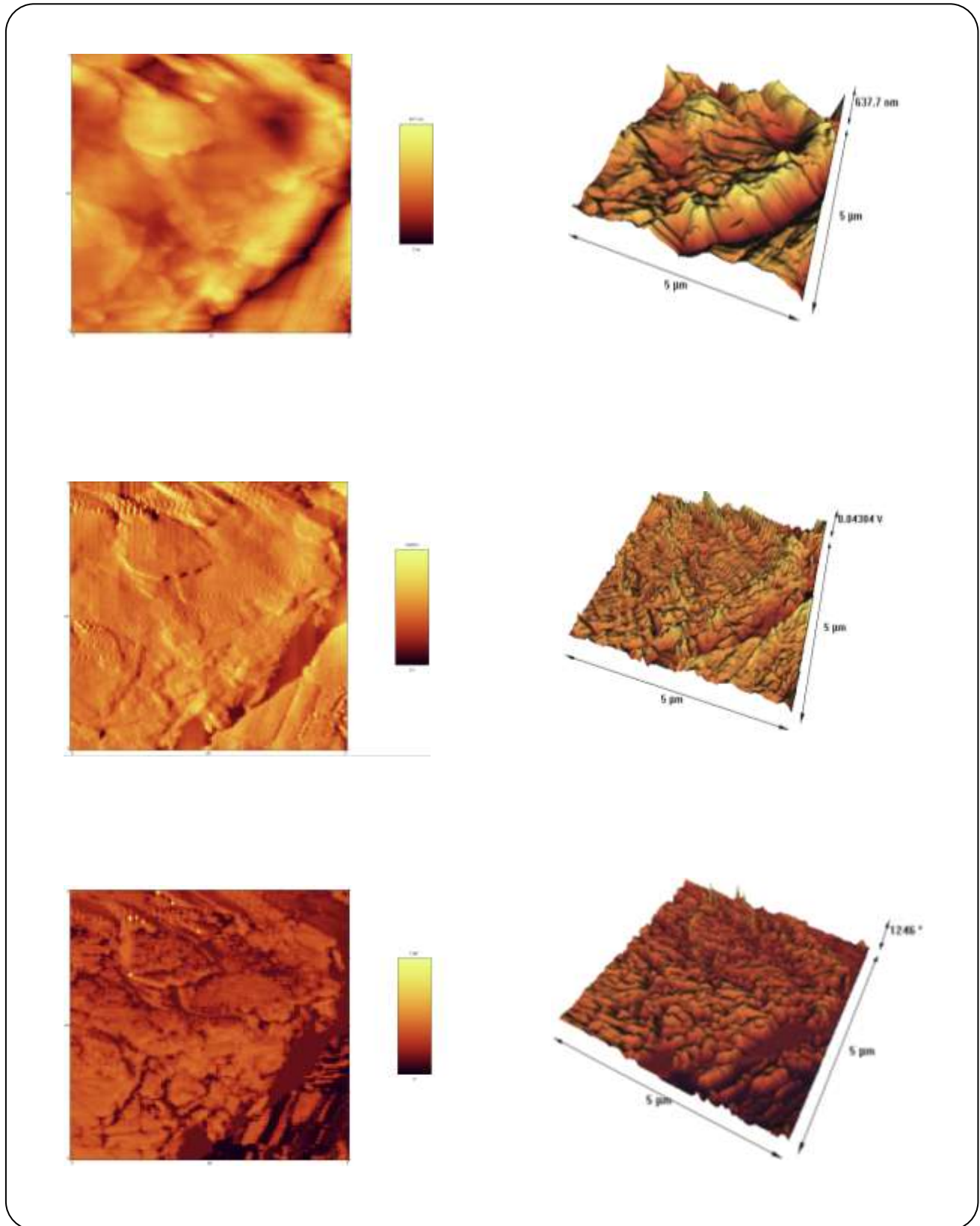
Fig. 4: AFM topographical, amplitude and phase images (A) 2D and (B) 3D (5×5 µm) for characterization surface Ni/POA/CPE.

Table 2: Effects of various parameters on the oxidation peak current density at the Ni/POA/CPE for
1.15 M ethanol + 0.1 M NaOH solution at υ = 20 mV/s.

C_{NiSO_4}/M	0.5	1	1.5	2	2.5
j_{pII}/mA cm^{-2}	1.02	1.64	1.89	1.85	1.79
t_a/s	5	10	20	30	60
j_{pII}/mA cm^{-2}	4.35	7.32	10.11	12.31	12.29
Cycle number	2	5	10	15	20
j_{pII}/mA cm^{-2}	0.2	0.25	0.35	0.11	0.05
C_{OA}/mM	0.5	1	2	4	6
j_{pII}/mA cm^{-2}	0.25	0.82	0.98	0.65	0.45

Fig. 5: Electrochemical responses of the (a) Ni/CPE and (b) Ni/POA/CPE in 1.78 M C₂H₅OH + 0.1 M NaOH solution at υ = 20 mV/s.
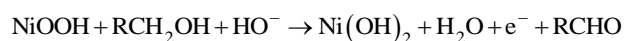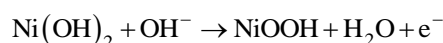
The results of quantitative measurements of surface roughness, such as mean roughness (R_a=13.94 nm) and mean roughness depth (R_z=82.46 nm) were achieved.

Electrocatalytic oxidation of ethanol

The typical CVs showing the electrooxidation of ethanol at the Ni/POA/CPE electrode are shown in Fig. 5. In all experiments, the working electrode was immersed in a 0.1M NaOH solution containing 0.05M ethanol. An increment in the anodic peak current for peak I followed by the appearance of a new peak II at more positive potential and a decrease of the cathodic peak current are the main effects observed upon the addition 0.05M ethanol to the electrolyte. As can be seen in Fig. 5, the peak current of ethanol oxidation at the surface of Ni/POA/CPE is about 1.43-fold greater than that at Ni/CPE. This behavior

is typical of that expected for mediated oxidation, as previously reported in the literature [29, 30]:

Electrooxidation process of ethanol in alkaline solution suggested by Fleischmann et al. [31, 33] that shows in below equation;

$$Ni(OH)_2 + OH^- \rightarrow NiOOH + H_2O + e^-$$

$$NiOOH + RCH_2OH + HO^- \rightarrow Ni(OH)_2 + H_2O + e^- + RCHO$$

$$RCHO + 3OH^- \rightarrow RCOO^- + 2H_2O + 2e^-$$

Parameters affecting the electrode modification

In order to evaluate the effects of various parameters such as NiSO$_4$ concentration (C_{NiSO_4}) , POA thickness, OA concentration (C_{OA}), and accumulation time (t_a) on ethanol oxidation, the anodic peak current density was monitored as an index for finding an optimum conditions and obtained results were summarized in Table 2. The data indicate that the peak current density increases extensively for C_{NiSO_4} up to 1.5M, t_a up to 1 min, cycle numbers up to 10, C_{OA} up to 2.0 mM and drop afterward.

Effect of ethanol concentration

Fig. 6 shows the effect of ethanol concentration on its electrooxidation current at the Ni(OH)$_2$/POA/CPE. It is clearly observed that the anodic peak current increases with increasing of ethanol concentration and drops afterward at higher concentrations. We assume this effect may be due to the saturation of active sites and/or poisoning the electrode surface with adsorbed intermediates. Thus, a concentration value of 1.99 M represents a critical concentration after which the adsorption of the oxidation products at the electrode surface causes the hindrance of further oxidation.
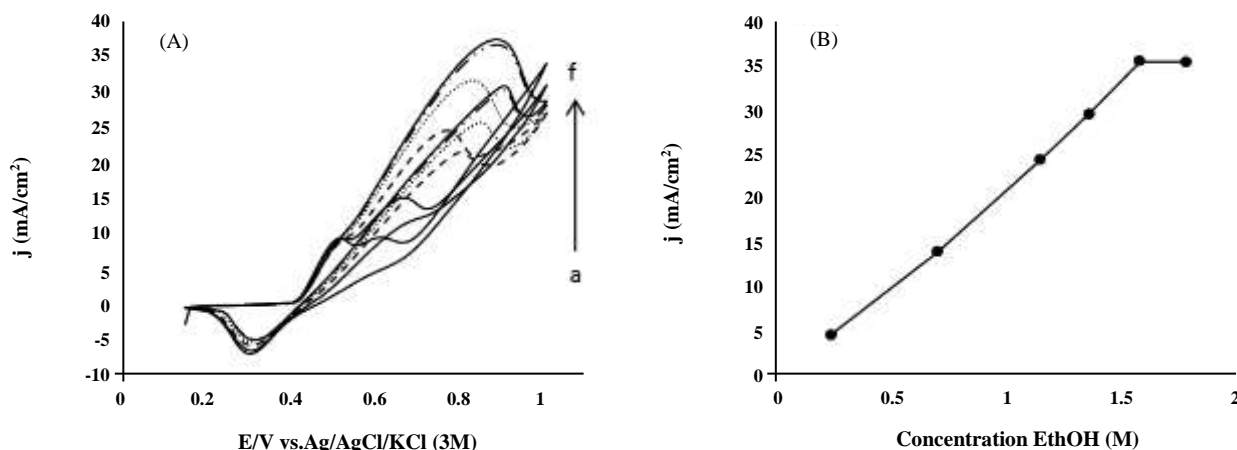
Fig. 6: (A)Current-potential curves of the Ni/POA/CPE in 0.1 M NaOH solution with different ethanol concentrations at
$v = 20$ mV/s: (a) 0.24, (b) 0.48, (c) 0.92, (d) 1.58, (e) 1.78 and (f) 1.99 M. (B) The j_{pII} as a function of C_2H_5OH concentration.

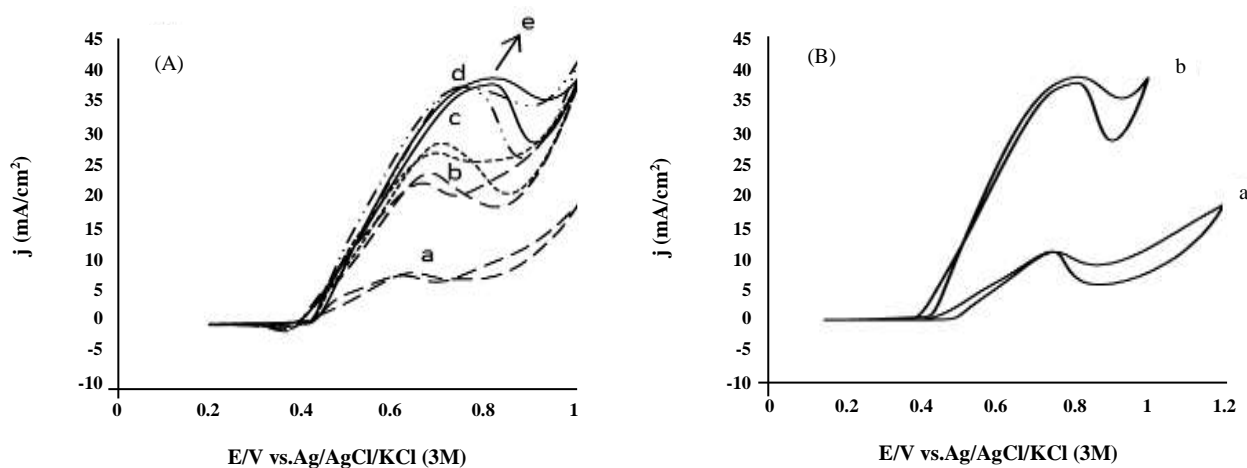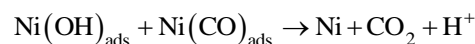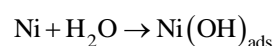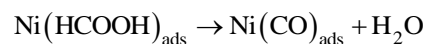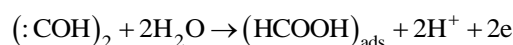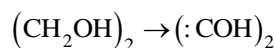**Fig. 7: (A) CVs of the Ni/POA/CPE in 0.1M NaOH solution with different ethylene glycol concentration**
a) 0.02, b)0.05, c)0.12, d)0.25 and e)0.52M, at $v = 20$ mV/s. (B) CVs of the (a) Ni/CPE and
(b) Ni/POA/CPE 0.1 M NaOH solution + 0.52 M ethylene glycol at $v = 20$ mV/s.

Electrocatalytic oxidation ethylene glycol

Our results show that ethylene glycol can be effectively catalyzed on the surface of Ni/POA/CPE. Fig. 7 shows the effect of ethylene glycol concentration on the anodic current of Ni/POA/CPE. It is clearly observed that the anodic current increases with increasing ethylene glycol concentration. As can be seen at lower concentration, the peak current observed for ethylene glycol is a little higher than ethanol, but for higher concentration its current levels off much sooner than that of ethanol due to the saturation of active sites on the surface of the electrode (ethylene glycol is a bulkier molecule with respect to ethanol). Finally, electrooxidation Ethylene glycol on the surface of Ni/POA/CPE produces formic acids. The mechanism for ethylene glycol oxidation would be as follow.

$$\left(CH_2OH\right)_2 \rightarrow \left(:COH\right)_2$$

$$\left(:COH\right)_2 + 2H_2O \rightarrow \left(HCOOH\right)_{ads} + 2H^+ + 2e$$

$$Ni\left(HCOOH\right)_{ads} \rightarrow Ni\left(CO\right)_{ads} + H_2O$$

$$Ni + H_2O \rightarrow Ni\left(OH\right)_{ads}$$

$$Ni\left(OH\right)_{ads} + Ni\left(CO\right)_{ads} \rightarrow Ni + CO_2 + H^+$$

Chronoamperometry study

Double potential step chronoamperometry was employed for investigation of electrochemical processes at the Ni/POA/CPE. Fig. 8A shows the double-step chronoamperograms of the modified electrode by setting the working electrode potential at 0.8 V (first step) and 0.47 V (second step) vs. reference electrode for various ethanol concentrations. In the presence of ethanol, the charge value associated with the forward chronoamperometry, Q_a, is greater than that backward chronoamperometry (Fig. 8B (h′)). This technique can also be used for evaluation of chemical reaction between ethanol and the modifier layer (catalytic rate constant, k) according to [32]:

$$I_C/I_L = \pi^{1/2}\lambda^{1/2} = \pi^{1/2}\left(kc_ot\right)^{1/2}$$

Where I_C and I_L are the currents in the presence and absence of ethanol, k is catalytic rate constant; C_o is the bulk concentration of ethanol and t is the elapsed time. From the slope of I_C/I_L vs. $t^{1/2}$ plot, presented in Fig. 8C, the mean value of k for concentration ranges 4.3-31.0 mM of ethanol was obtained as about 2.6×10^6 cm^3/mol.s. According to the method described above, the value of k for ethylene glycol was found to be 1.07×10^7 cm^3/mol.s. The higher k value for ethylene glycol can be attributed to the fact that it is a diol.

Stability of the Ni/POA/CPE

In the practical view, long-term stability of the electrode is important. The long-term stability of Ni/POA/CPE was examined in 0.1 M NaOH + 48.0 mM ethanol solution by using CV technique (Fig. 9A). The peak current density decreases gradually by continuous potential cycling and its value at the 50th scan is about 73% than the 1st scan. For further evaluate the activity and stability of the Ni/POA/CPE, chronoamperogram (CA) were recorded for a large time window in the presence of ethanol (Fig. 9B). As can be seen, the decrease in current is relatively slow. It is obvious that the Ni/POA/CPE exhibits a good stability toward ethanol oxidation. We also checked the stability of the modified electrode by measuring its response to ethanol oxidation after 30 days of storage in the laboratory atmosphere condition (Figure not shown). The electrode response to electrocatalytic oxidation of ethanol retains 85% of initial value. In comparison with some other previous works,
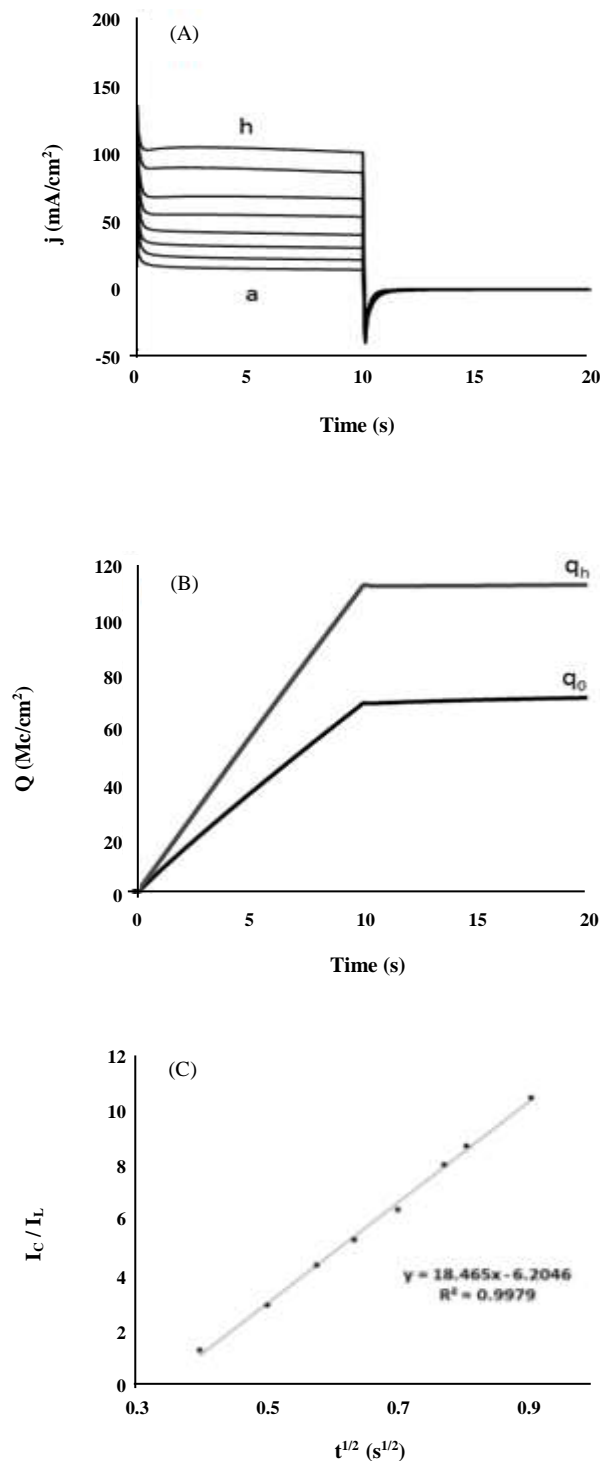

Fig. 8 : (A) CVs obtained at the Ni/POA/CPE in the absence (a) and the presence of (b) 4.3, (c) 9.2, (d) 14.0, (e) 18.0, (f) 22.0, (g) 27.0 and (h) 48 mM ethanol. (B) The dependency of charge Q vs. t derived from the data of chronoamperogram of (a) and (j). (C) The dependency of I_C/I_L on $t^{1/2}$ derived from the data of chronoamperograms of (a) and (j) in the main panel.
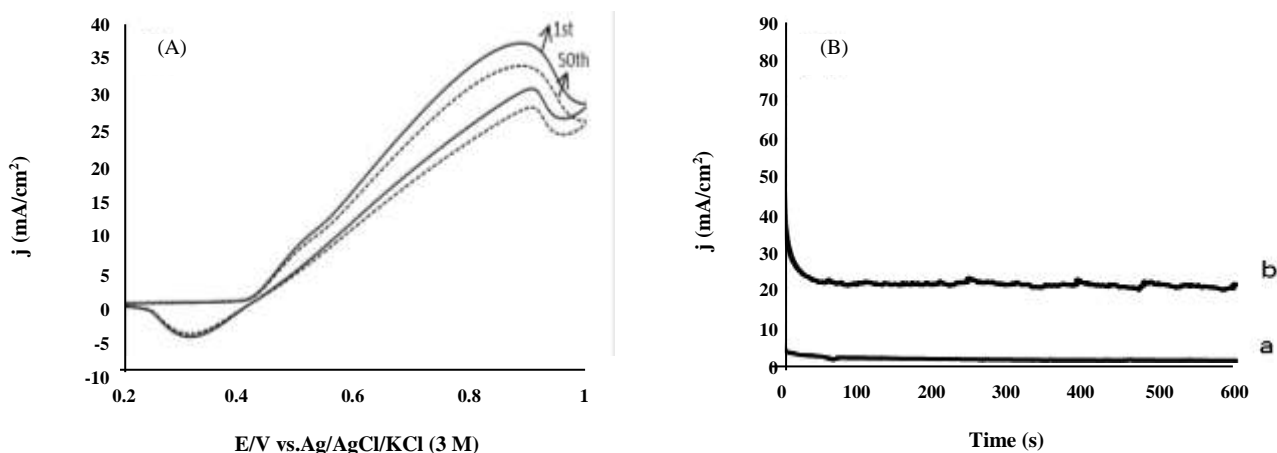
Fig. 9: (A) CVs of the Ni/POA/CPE in the presence of 2.78 M ethanol in 0.1 M NaOH solution: 1st cycle (a); 50th cycle (b) at υ = 20 mV/s. (B) chronoamperogram of the Ni/CPE (a) and Ni/POA/CPE (b) in 2.78 M C_2H_5OH + 0.1 M NaOH solution.

it seems clear that nickel hydroxide in the modified electrode can act as a comparable catalyst in ethanol oxidation.

CONCLUSIONS

In this paper, a poly (o-Anisidine) film prepared at the surface of carbon paste electrode. By using accumulation method nickel particles stabilized on the polymer surface. Modified electrode showed a good electrocatalysis for ethanol and ethylene glycol.

Using conductive polymer showed less charge transfer resistance in comparison with unmodified carbon paste electrode.

Choronoamperometric method was used to calculate the catalytic rate constants for ethanol and ethylene glycol approximately.

In electrooxidation process of ethanol in alkaline solution, Ni/POA/CPE is indicated a good stability to use in direct ethanol fuel cells.

REFERENCES

[1] Antolini E., Gonzalez E.R., Alkaline Direct Alcohol Fuel Cells, *J. Power Sour*, **195** (11): 3431-3450 (2010).

[2] Lamy C., Belgsir E.M., Léger, J.M., Electrocatalytic Oxidation of Aliphatic Alcohols: Application to the Direct Alcohol Fuel Cell (DAFC), *J. Appl. Electrochem*, **31** (7): 799-809 (2001).

[3] Kamarudin M.Z.F., Kamarudin S.K., Masdar M.S., Daud W.R.W., Review: Direct Ethanol Fuel Cells, *International Journal of Hydrogen Energy*, **38**(22): 9438-9453 (2013).

[4] Liu B., Chen J.H., Zhong X.X., Cui K.Z., Zhou H.H., Kuang Y.F., Preparation and Electrocatalytic Properties of Pt–SiO$_2$ Nanocatalysts for Ethanol Electrooxidation, *J. Coll. Int. Sci*., **307** (1): 139-144 (2007).

[5] Livshits V., Peled E., Progress in the Development of a High-Power, Direct Ethylene Glycol Fuel Cell (DEGFC), *J. Power Sour*., **161** (2): 1187-1191 (2006).

[6] Livshits V., Philosoph M., Peled E., Direct Ethylene Glycol Fuel-Cell Stack-Study of Oxidation Intermediate Products, *J. Power Sour*., **178** (2): 687-691 (2008).

[7] Matsuoka K., Inaba M., Iriyama Y., Abe T., Ogumi Z., Matsuoka M., Anodic Oxidation of Polyhydric Alcohols on a Pt Electrode in Alkaline Solution, *Fuel. Cell.*, **2** (1): 35-39 (2002).

[8] Matsuoka K., Iriyama Y., Abe T., Matsuoka M., Ogumi Z., Alkaline Direct Alcohol Fuel Cells Using an Anion Exchange Membrane, *J. Power Sour.*, **150**: 27-31 (2005).

[9] Shen S.Y., Zhao T.S., Wu Q.X., Product Analysis of the Ethanol Oxidation Reaction on Palladium-Based Catalysts in an Anion-Exchange Membrane Fuel Cell Environment, *Int. J. Hydrogen Energy*, **37** (1): 575-582 (2012).

[10] An L., Zhao T.S., Xu J.B., A Bi-Functional Cathode Structure for Alkaline-Acid Direct Ethanol Fuel Cells, *Inte. J. Hydrogen Energy*, **36** (20): 13089-13095 (2011).

[11] Antolini E., Catalysts for Direct Ethanol Fuel Cells, *J. Power Sour*, **170** (1): 1-12 (2007).

[12] Christensen P.A, Hamnett A., The Oxidation of Ethylene Glycol at a Platinum Electrode in Acid and Base: An in Situ FT-IR Study, *J. Electroanal. Chem. Inter. Electrochem*, **260** (2): 347-359 (1989).

[13] Beden B., Kadirgan F., Kahyaoglu A., and Lamy C., Electrocatalytic Oxidation of Ethylene Glycol in Alkaline Medium on Paltinum-Gold Alloy Electrodes Modified by Under Potential Deposition of Lead Adatoms, *J. Electroanal. Chem. Inter. Electrochem*, **135** (2): 329-334 (1982).

[14] Habibi E., Razmi H., Kinetics of Direct Ethanol Fuel Cell Based on Pt-PoPD nano Particle Anode Catalyst, *Int. J. Hydrogen Energy*, **38** (13): 5442-5448 (2013).

[15] Song S., Wang Y., Shen P., Thermodynamic and Kinetic Considerations for Ethanol Electrooxidation in Direct Ethanol Fuel Cells, *Chinese. J. Catal*, **28**(9): 752-754 (2007).

[16] Zhu M., Sun G., Li H., Cao L., Xin Q., Effect of the Sn(II)/Sn(IV) Redox Couple on the Activity of PtSn/C for Ethanol Electro-oxidation, *Chinese. J. Catal*, **29** (8): 765-770 (2008).

[17] Erini N., Krause P., Gliech M., Yang R., Huang Y., Strasser P., Comparative Assessment of Synthetic Strategies Toward Active Platinum–Rhodium–tin Electrocatalysts for Eficient Ethanol Electro-Oxidation, *J. Power Sour*, **294**: 299-304 (2015).

[18] Wang C., Ren F., Zhai C., Zhang K., Yang B., Bin D., Wang H., Yanga P., Du Y., Au-Cu-Pt Ternary Catalyst Fabricated by Electrodeposition and Galvanic Replacement with Superior Methanol Electrooxidation Activity,*RSC. Adv.*, **4** (101): 57600-57607 (2014).

[19] Xia B.Y., Wu H.B., Wang X., Lou X.W., One-Pot Synthesis of Cubic PtCu3 Nanocages with Enhanced Electrocatalytic Activity for the Methanol Oxidation Reaction, *J. American Chem. Soc.*, **134** (34): 13934-13937 (2012).

[20] Lee E., Park I.S., Synthesis and Characterization of Pt−Sn−Pd/C Catalysts for Ethanol Electro-Oxidation Reaction, *J. Phys. Chem. C*, **114** (23): 10634-10640 (2010).

[21] Ahmed M.S., Jeon S., New Functionalized Graphene Sheets for Enhanced Oxygen Reduction as Metal-Free Cathode Electrocatalysts, *J. Power Sour*, **218**: 168-173 (2012).

[22] Dutta A., Datta J., Energy Efficient Role of Ni/NiO in PdNi Nano Catalyst Used in Alkaline DEFC, *J. Mat. Chem. A*, **2** (9): 3237-3250 (2014).

[23] Ojani R., Raoof J.B., Rahemi V., Evaluation of Sodium Dodecyl Sulfate Effect on Electrocatalytic Properties of Poly (4-Aminoacetanilide)/Nickel Modified Carbon Paste Electrode as an Efficient Electrode Toward Oxidation of Ethylene Glycol, *Int. J. Hydrogen Energy*, **36** (20): 13288-13294 (2011).

[24] Barbosa A.F.B., Oliveira V.L., van Drunen J., Tremiliosi-Filho G., Ethanol Electro-Oxidation Reaction Using a Polycrystalline Nickel Electrode in Alkaline Media: Temperature Influence and Reaction Mechanism, *J. Electroanal. Chem.*, **746**: 31-38 (2015).

[25] Ureta-Zañartu M.S., Alarcón A., Muñoz G., Gutiérrez C., Electrooxidation of Methanol and Ethylene Glycol on Gold and on Gold Modified with an Electrodeposited polyNiTSPc Film, *Electrochim. Acta.*, **52** (28): 7857-7864 (2007).

[26] Liu Z., Li Z., Wang F., Liu J., Ji J., Wang J., Wang W., Qin S., Zhang L., Qin L.Z., Synthesis of Multi-Walled Carbon Nanotube Supported Nickel Catalysts by Hydrazine Reduction and Their Electrocatalytic Activity on Ethanol Electro-Oxidation, *Mat. Letters*, **65** (23–24): 3396-3398 (2011).

[27] Rice M.E., Galus Z., Adams R.N., Graphite Paste Electrodes: Effects of Paste Composition and Surface States on Eectron-transfer Rates, *J. Electroanal. Chem. Inter. Electrochem*, **143** (1–2): 89-102 (1983).

[28] Ojani R., Raoof J B., Zamani S., A Novel Sensor for Cephalosporins Based on Electrocatalytic Oxidation by Poly(o-anisidine)/SDS/Ni Modified Carbon Paste Electrode, *Talanta*, **81** (4–5): 1522-1528 (2010).

[29] Raoof J.B., Ojani R., Hosseini S.R., An Electrochemical Investigation of Methanol Oxidation on Nickel Hydroxide Nanoparticles, *South African J. Chem.*, **66**: 00-00 (2013).

[30] Ojani R., Raoof J.B., Hosseini S.R., Electrocatalytic Oxidation of Methanol on Carbon Paste Electrode Modified by Nickel Ions Dispersed Into Poly (1,5-Diaminonaphthalene) Film, *Electrochim. Acta*, **53** (5): 2402-2407 (2008).

[31] Ghasemi S., Hosseini S.R., Asen P., Preparation of Graphene/Nickel-Iron Hexacyanoferrate Coordination Polymer Nanocomposite for Electrochemical Energy Storage, *Electrochim. Acta,* **160**: 337-346 (2015).

[32] Bard A.J., Faulkner L.R., "Electrochemical Methods: Fundamentals and Applications", Wiley and Sons, New York, (2001).

[33] Fleischmann M., Korinek K., Pletcher D., The Oxidation of Hydrazine at a Nickel Anode in Alkaline Solution, *J. Electroanal. Chem. Inter. Electrochem*, **34** (2): 499-503 (1972).

[34] Dailey D., Jungwon S., Korzeniewski C., Ethylene Glycol Electrochemical Oxidation at Platinum Probed by Ion Chromatography and Infrared Spectroscopy, *Electrochimi. Acta.*, **44** (6–7): 1147-1152 (1998).